WARSAW UNIVERSITY OF TECHNOLOGY Index 351733
FACULTY OF CIVIL ENGINEERING
COMMITTEE FOR CIVIL AND WATER ENGINEERING
POLISH ACADEMY OF SCIENCES ISSN 1230-2945

DOI: 10.24425/ace.2021.138511

ARCHIVES OF CIVIL ENGINEERING

Vol. LXVII ISSUE 4 2021

pp. 451 –467

Research paper

Generating 3D point-cloud based on combining adjacent multi-station scanning data in 2D laser scanning: A case study of Hokuyo UTM 30lx

Anh Thu Thi Phan[1,2], Ngoc Thi Huynh[3,2]

Abstract: Using a lower-cost laser scanner for generating accuracy in 3D point-cloud has been a concern because of economic issues; therefore, this study aims to create a 3D point cloud of a target object using a low-cost 2D laser scanner, Hokuyo UTM 30LX. The experiment was carried out in November 2019 with 16 single scans from 8 different viewpoints to capture the surface information of a structure object with many intricate details. The device was attached to a rail, and it could move with stable velocity thanks to an adjustable speed motor. The corresponding 16 point-clouds were generated by using the R language. Then, they were combined one by one to make a completed 3D point cloud in the united coordinate system. The resulted point cloud consisted of 1.4 million points with high accuracy (RMSE = ±1.5 cm) is suitable for visualizing and assessing the target object thanks to high dense point-cloud data. Both small details and characters on the object surface can be recognized directly from the point cloud. This result confirms the ability of generated the accuracy point cloud from the low-cost 2D laser scanner Hokuyo UTM 30LX for 3D visualizing or indirectly evaluating the current situation of the target object.

Keywords: 2D laser scanner, 3D point cloud, visualization, LiDAR technology

[1]PhD., Eng., Anh Thu Thi Phan, Department of Geomatics Engineering, Faculty of Civil Engineering, Ho Chi Minh City University of Technology, 268 Ly Thuong Kiet Street, District 10, Ho Chi Minh City, Vietnam, e-mail: ptathu@hcmut.edu.vn, ORCID: 0000-0003-2778-9139

[2]Vietnam National University Ho Chi Minh City, Linh Trung Ward, Thu Duc District, Ho Chi Minh City, Vietnam

[3]PhD., Eng., Thi Huynh Ngoc, Department of Bridge and Highway Engineering, Faculty of Civil Engineering, Ho Chi Minh City University of Technology, 268 Ly Thuong Kiet Street, District 10, Ho Chi Minh City, Vietnam, e-mail: huynhngocthi@hcmut.edu.vn, ORCID: 0000-0003-0192-1592

1. Introduction

LiDAR scanning technology has been popularly used in various fields for many purposes, such as civil; architecture; archeology; agriculture; transportation; and military applications [1–4]. Terrestrial Laser Scanner (TLS) is handy to virtually rebuild the historical heritage because this laser scanning technique does not damage the object due to non-touch interaction in the scanning stage [5, 6]. Moreover, LiDAR technology helps construction management, such as evaluating the building's status [7, 8]. Scan to BIM proposes a helpful technique for the near future in building and managing construction information [9–12]. For this technique, thousands of scanning points can be collected in a single second. As a result, a dense point cloud that captures the object's shape can be created by one scan in several minutes.

A point cloud, popularly known as a set of data points in space, represents an object's 3D shape. Each point has its coordinate in a 3D dimensional coordinate system. Using point cloud for 3D representation came into popularity recently due to the fact that point clouds can display 3D images of a given object with high resolution [13, 14]. Moreover, the point cloud can be used for reconstructing the 3D model of the objects [15, 16]. However, a significant problem in generating point clouds is the complexity of point clouds and 3D objects in the real world.

The image-matching method merits consideration as a promising solution. Because of low operation and hardware costs, and the development of many types of low altitude UAVs, UAV aerial photogrammetry has been applied in many application areas [18–22]. The image-based point clouds are utilized like laser scanner-based point clouds or used together [23–26]. However, the accuracy of the image-based point clouds depending on the image processing algorithm and image quality. The generated point clouds also contain many noisy points.

Precise 3D point clouds can be generated by utilizing a Terrestrial Laser Scanner (TLS). Their advantages have been mentioned in many types of research [27, 28]; Therefore, surveying and mapping work have been more comfortable due to the continuous development of new technology, primarily 3D technology. However, cost is the largest concern surrounding the utilization of laser devices. A 3D laser scanner that can produce good quality and detailed visualization of the point cloud is very high; however, the cost can vary from tens to hundreds of thousands of dollars for a single device. Such devices are uneconomical for small projects in developing countries. Using a device that costs a few several thousand dollars can be considered a good solution for applying LiDAR scanning technology because of the limited cost.

This research aims to evaluate the ability to generate accurate 3D point clouds using a low-cost 2D laser scanner. The research's goal is to create a 3D point cloud that describes the geometry shape of the object's surface using a 2D laser scanner which is not designed for surveying purposes. For collecting data, the Hokuyo UTM 30LX laser scanner is used. This device's cost is only 3500 dollars and many times as cheap as a standard 3D laser scanner. Three main problems need to be solved to achieve the research objective: (i) creating a 3D point cloud from the nadir and oblique scanning, (ii) registering data from multi-scanning stations, and (iii) evaluating the quality of the resulted point-clouds. In general, a 3D terrestrial laser scanner quickly obtains a full image of the object's surface in experimental conditions because it can rotate 360 degrees. The emitter is mounted on a device's body that contains a mirror that reflects the laser and directs it toward the point detected; however, the 2D laser scanners collect data in the scanning line. The device and the object must have relative movement to obtain an

image of the respective surface. In other words, to create a 3D point cloud of an object using a 2D laser scanner, either the device moves or the device is fixed and the object moves. In this study, to solve the data collecting problem, the device is mounted on a frame and moves under the motor's power. The target object would be observed in different positions by the scanner to get the full image of the object. Then, many point clouds will be fused to make a complete image of the object. For each station, both nadir and oblique scanning is performed to capture data. Thus, the tilt angle of the scanning plane needs to be adjusted before incorporating both the nadir and oblique scan data together.

The registration of clouds to create a complete point cloud of the object is done sequentially for each station, after which the data of all stations is linked together. This process is carried out by identifying four tie points to solve the affine transformation model parameters. The evaluation of the model's accuracy is done through direct measurement and the measurement results on the point cloud. This study's expected result is the complete 3D point cloud of the target object that can be visualized the object's surface in detail and accuracy. Recently, many open-source tools and software have become available. They are supported for point cloud processing. Therefore, using a non-survey grade laser scanner for generating a 3D point cloud has become a more feasible option.

2. The experiment

2.1. System description

The device used in this research is a non-survey-grade laser scanner – Hokuyo UTM 30LX. It is a 2D laser scanning range finder that captures distances and reflectance intensity in a plane. The laser scanner uses the principle of distance measurement, in which a laser pulse is sent out and reflected from a target object's surface. Then, it returns to the device. The time-of-flight principle obtains the distance. The used laser scanner is a lightweight, compact device. In detail, its external dimension ($W \times D \times H$) is $60 \times 60 \times 85$ mm with a weight of only 370 g. The field of view is 270° with an angular resolution of 0.25°, which results in 1080 distance measurements per line during 25 milliseconds. The device uses a wavelength of 905 nm. It can detect an object in a range of 0.1 m up to 30 m with an accuracy of 30 mm to 50 mm. The minimum width saw at 10 m is 130 mm. The detailed specification of the scanner given by the distributor is summarized in Table 1.

The 2D laser scanner collects data in line; therefore, the scanner must move along the target object to get the complete surface information of the target's surface. For this reason, the continuous and stable movement will give the best data quality. The scanner is mounted on an aluminum frame. An adjustable speed motor is equipped behind the frame and drives the device through a rubber transmission system with slightly annual vibration from the device's movement. As a result, the device can move along the rail with 1.5 m of length. The moving velocity can be set as a constant by a speed controller (Fig. 1). However, the target object may be taller than the installation height of the device. In this case, the scanning plane can be adjusted by rotating the aluminum plate. The laser scanner is mounted to capture data in the oblique scanning with different oblique angles.

Table 1. Main specification of 2D Laser scanner Hokuyo UTM 30LX

Model No.	UTM-30LX
Prices	3500 USD
Power source	12 V DC ±10% (Current consumption: Max: 1 A, Normal: 0.7 A)
Light source	Semiconductor laser diode (λ = 905 nm) Laser safety Class 1(FDA)
Detection Range	0.1 to 30 m (White Square Kent Sheet 500 mm or more), max. 60 m
Accuracy	0.1 to 10 m: ±30 mm, 10 to 30 m: ±50 mm[*1]
Scanning time	25 ms
Field of view	Up to 270°
External dimension (W × D × H)	60 × 60 × 85 mm
Weight	370 g

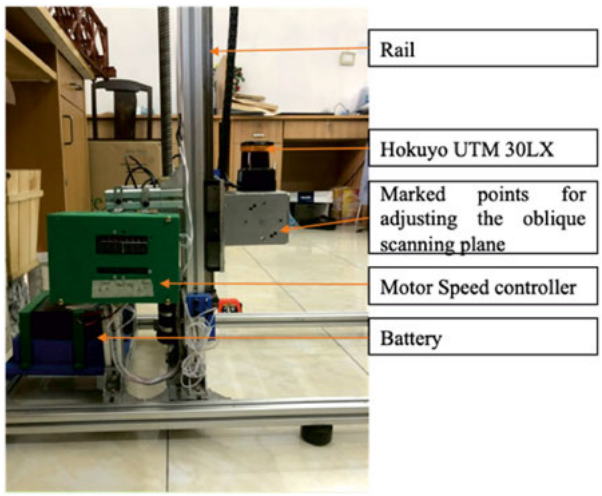

Fig. 1. Illustration of the laser scanner system. The Hokuyo UTM 30LX laser scanner is mounted on an aluminum frame. It can move along the rail under motor power

2.2. Testing object

For collecting data conveniently, an object located at the Vietnam National University campus- Ho Chi Minh University of Technology, Vietnam is chosen. Its structure is complex, with many angles and details (Fig. 2). This object can be separated into three parts: base, head, and body. It is approximate 2.2 meters in height and 0.7 meters in width of the head portion. The base is flat and has a gear shape with nine teeth. The body reduces in size from the base to 45 cm in height, where it increases in size again. Many bumps around the body can be visualized clearly. The head has four prominent faces with different shapes. Each face is almost flat with many small humps and bumps to make the decorating details. There are many characters arranged on the object's surface. It is challenging to directly measure all of the details to get a precise overview of the object.

Fig. 2. The target object located at the campus of Ho Chi Minh City University of Technology-VNU. This object includes three main parts (base, body, and head) with many intricate details on its surface

2.3. Data acquisition

The using laser scanner, Hokuyo UTM30 LX, is a single beam 2D laser scanner in this study. When a laser pulse hits the object, it will return to the device. The object surface's contact position is recorded as one scanning point, which will be identified based on the scanning angle and range value. The laser pulse cannot go past the object. It is clear that in one scan, only the front surface of the object can be captured. The rest of the object, hidden, cannot be captured because of the target object's complex shape. Therefore, to get the entire data for visualizing a 3D image of the object, data must be collected in many stations.

Moreover, the head's particular shape is the combination of 4 surfaces with four right angles. The scanner must be set in front of those surfaces and corners to get the good quality in details of point clouds. As a result, eight stations were set up in front of four faces and four corners of the head, at an observed distance of approximately 2.0 meters (Fig. 3).

As mentioned above, the data is capture in a plane by using a 2D laser scanner. For getting the whole image of the target object, the scanner must move along the rail under the support of motor power. Moreover, the length of rail is limited. It is shorter than the height of the target object; hence, it is necessary to change the scanning plane's position for getting data that can cover the upper or lower part of the object from the horizontal line in nadir scanning.

The experiment was carried out on a shady day in November of 2019. Many 3M reflective stickers made of PMMA top film layer giving high reflectance were attached to the object's surface for combining data to collect data fully. Eight positions around the object mentioned above were chosen to set the devices. From that position, the scanner could capture the entire surface of the object. The scanner is set to move vertically. The controller can adjust the settling velocity. In this experiment, the setting speed is 2.0 cm/s (Fig. 3). The laser scanner could record 40 scan lines per second, each with 1080 distance and intensity measurements for 270 degrees of field of view. For this study, to reduce the number of useless points, the 180 degrees

Fig. 3. Data acquisition at one viewpoint. (a) The device moves along the rail from the bottom to capture the image of the object. (b) Illustration nadir and (c) oblique scanning

of view is set by the UrgBenri Plus application; therefore, each scan line contains 720 scan points. For collecting the data, the base and body parts are captured in nadir scanning. Because the head part is out of reach in nadir scanning, the scanning plane has adjusted an angle of 30 degrees upward from the horizontal plane to capture data. As a result, 16 raw files (*.ubh file) are recorded. They correspond to 4 faces and four corners of the object in the nadir and oblique scanning plane. Besides the collected laser data, the size of 20 details of the object is also be measured directly to evaluate the accuracy of the generated point cloud (Fig. 4). The measured result is displayed in detail in Table 2.

Table 2. The size of 20 details of the object

ID	Directly measured length (cm)	ID	Directly measured length (cm)
1	0.5	11	126.5
2	51.0	12	2.5
3	44.0	13	26.0
4	26.8	14	17.5
5	26.5	15	82.2
6	9.9	16	10.0
7	1.0	17	10.5
8	21.5	18	44.0
9	7.5	19	6.0
10	98.0	20	11.0

Fig. 4. The direct measurement is performed for determining the size of the object. The ID of each detail is numbered

3. Data processing

This paper describes our experiments concerning the generation of accuracy 3D point cloud using 2D laser scanner Hokuyo UTM 30LX. In particular, this section describes 3D point clouds' workflow generating from the raw files (*.ubh file). Then, adjacent multi-station point clouds would be registered by aligning the correspondent point clouds. Those point clouds are combined and displayed in the same coordinate system. Finally, the resulting point cloud's accuracy is evaluated by checking the visualization and comparing it with the direct measurements.

3.1. Point cloud generation from a single scan

For 3D point cloud generation from data collected by a 2D laser scanner, the first step is converting measured polar coordinates (distance D, horizontal angle θ, and oblique angle φ) into the local laser scanner coordinate system for each scanning line. The laser scanner coordinate system is assumed as a right-hand coordinated system with the origin point located at the device's reflector mirror (Fig. 5). This coordinate system is based on the scanning plane and the direction of the device's movement. In detail, the X-axis is parallel to the slider and point to the direction of movement. The Z-axis is perpendicular to the scanning plane, and its

positive direction coincides with gravity. The right-hand rule determines the Y-axis. Therefore, the coordinates of the points in the point cloud can be calculated using the formula (3.1):

$$\begin{aligned} x^{LS} &= r \cdot \sin\varphi \cdot \cos\theta \\ y^{LS} &= r \cdot \sin\theta \\ z^{LS} &= r \cdot \cos\theta \end{aligned} \tag{3.1}$$

where: $\left(x^{LS}, y^{LS}, z^{LS}\right)^T$ – 3D coordinate of a point in laser scanning coordinate system, r – scan range (m), θ – scan angle (degree), φ – oblique angle of the scanning plane.

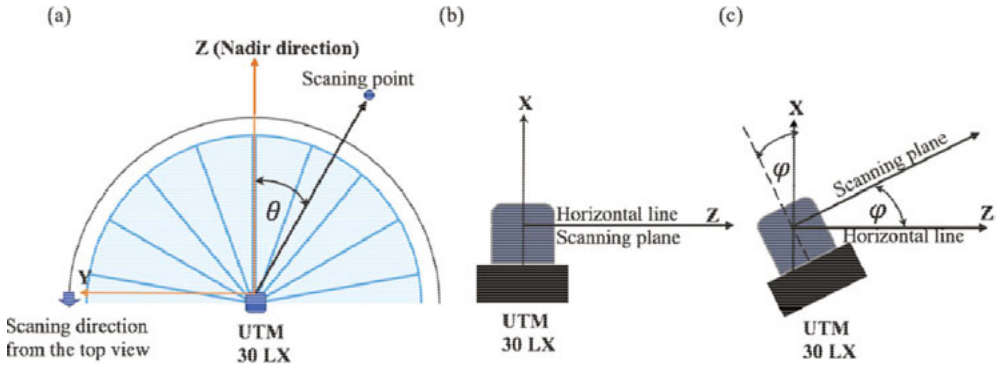

Fig. 5. The laser coordinate system. (a) Illustration of the location of scanning point in laser coordinate system top view. The laser coordinate system from slide view in (b) nadir scanning and (a) oblique scanning. The scanning angle is measured from the nadir direction to both sides. The nadir direction is considered as 0 degrees of scanning angle

According to equation (3.1), in the case of nadir scanning, all points have x^{LS} of 0 because of 0 degrees of oblique angle φ. Then, the X value was transformed to a new coordinate with the false origin located at the device's starting position on the rail. The X coordinate of each scanning plane is estimated and adjusted to the previouslyc-omputed value based on the set velocity. In this way, each scan line will be displayed as a horizontal row on the point cloud. The resulting dense point cloud is organized as non-overlapping scan lines. As a result, the 3D point cloud for one scan is generated. This point cloud will describe the image of objects at one specific viewpoint.

$$\begin{aligned} x &= x^{LS} + v \cdot t \\ y &= y^{LS} \\ z &= z^{LS} \end{aligned} \tag{3.2}$$

where: $(x, y, z)^T$ – 3D coordinate of a point in an assumed coordinate system for each scan, $\left(x^{LS}, y^{LS}, z^{LS}\right)^T$ – 3D coordinate of a point in laser scanning coordinate system, v – scan speed (m/s), t – travel time of scanner (s).

For this process, the range value is the primary information (Eq. 3.1). However, the raw file contained many data, such as range, intensity, scanning log time, and timestamp. The *.ubh

file is a generic file that contains sensor information and data. They include the header and data section with a mix of numerical and alphabetical format, and the data section has blocks corresponding to each scan cycle. Each scan cycle has a timestamp of the scan from the sensor, the log time, and scan data of the corresponding timestamp. A semi-colon separates the scan block; each scan block's intensity separator is a vertical bar. This led to difficulty in further analysis. The main problem of this process is to extract the range data from the *.ubh file. Therefore, the raw files must be detached to access a specific data type for each scanning point. The value of intensity, range data, and log time were then separated and saved to different text files for further analysis. For this, a script is developed in the R language. Then, raw files were read. Range and intensity data are saved to different text files. The range data is used to generate the 3D coordinates of all scanning points by considering the scanning angle, the scanning plane's tilt angle, and the scanner's movement speed as the mentioned process.

3.2. Registering data from multi-scanning stations

As mentioned above, the target object was obtained from eight viewpoints. In each viewpoint, both nadir and oblique scanning were carried out. In total, this experiment contained 16 separate scans, and 16 point clouds are correspondingly generated. They have outlier and noisy points because of the large setting field of view. They are also partially overlapped because they described the same object from different viewpoints. However, they are displayed in other independent 3D coordinate systems. Those point clouds needed to be registered to generate a resulted point cloud in a united coordinate system. In detail, The outlier of 16 point clouds is manually removed to reduce the data size. Then, two point clouds of each viewpoint are aligned by applying an affine transformation (eq. 3.3). For this, at least three tie points are required to compute the translation, rotation, and scale parameters. It means that one reference system will become the primary, and all other points will recompute the new coordinate in the primary system. In this study, four tie points should be selected to ensure the accuracy of the transformation process. Then, the least square method is applied to compute seven transformed parameters. The reflectance targets that signalize tie points are measured from adjacent scans to combine the data acquired at each viewpoint. Because of the object's complex shape, several specific positions on the object's surface are also chosen for this transformation process. This process is done from all viewpoints. Finally, eight point clouds corresponding to eight views are aligned by applying the same process. The main goal of this process is to set up a common reference system for whole point clouds.

$$\begin{bmatrix} x \\ y \\ z \end{bmatrix}^{primary} = \begin{bmatrix} T_x \\ T_y \\ T_z \end{bmatrix} + s \cdot R(\varphi, \lambda, \omega) \begin{bmatrix} x \\ y \\ z \end{bmatrix}^{reference} \tag{3.3}$$

where:

$\begin{bmatrix} x \\ y \\ z \end{bmatrix}^{primary}$ – denote the coordinates of a point in the primary coordinate system,

$\begin{bmatrix} x \\ y \\ z \end{bmatrix}^{reference}$ – indicate the coordinates of a point in the reference coordinate system,

$\begin{bmatrix} T_x \\ T_y \\ T_z \end{bmatrix}$ – denote the translation parameters,

s – scalling factor, $R(\varphi, \lambda, \omega)$ – denote the rotation matrix of three rotation angle in x-, y- and z-axis.

3.3. Evaluating the quality of resulted point cloud

The point cloud quality is evaluated through several factors such as point density, detail, distortion, clarity of detail of the objects, and the dimensional accuracy of each part. The point density is computed based on the average distance between points in each scan line and the moving speed of the device. The distortion and granularity of the objects are determined directly on each point cloud. The dimensional accuracy of the cloud is checked through the results of direct measurements and measurements on the point cloud. Twenty details have been measured for the evaluated process (Table 2). Finally, the root mean square error is computed to accurately measure the point cloud regarding the object's geometry.

4. Results

By following the data processing, 16 dense point clouds are created from 16 single scans of data. 8 point clouds are generated from nadir scanning data, and the remaining 8 point clouds are generated from oblique scanning data. They are referenced to different coordinate systems. Each point cloud contains approximately 280.000 points. With the moving velocity of 2 cm/s, the line distance is approximately 0.5 cm. The point spacing in one scan line is approximate 1.0 cm at the observed length of 2 m. Therefore, the estimated point density is two hundred thousand points per square meter. With such a dense point density, the point cloud is expected to display enough detailed object elements. Then the object's concrete surface will more or less affect the reflectivity of the scan points. It can affect the clarity of objects in 3D visualization. The experiment was conducted in the afternoon when it was shady, so most point clouds show similar reflectance values. The difference in the intensity of reflections on the object's surface helps to show the details of the object clearly (Fig. 6).

In general, the point cloud character can be read directly in a single scan; each minor character with 5 mm in width is also displayed clearly (Fig. 6a). The hump parts with a height of 1 cm also are captured. The captured point cloud has a scale of 1:1. Several features on the object measured on the point cloud are compared to the directly measured value. As a result, two details cannot be observed from the point cloud because of errors caused by oblique scanning. On both sizes, the point cloud and the object, the rest of the details are similar (Fig. 7). The errors were computed by taking the difference between measured data on the point cloud and the directly measured data. As a result, the maximum error of 2.4 cm is obtained for the detail

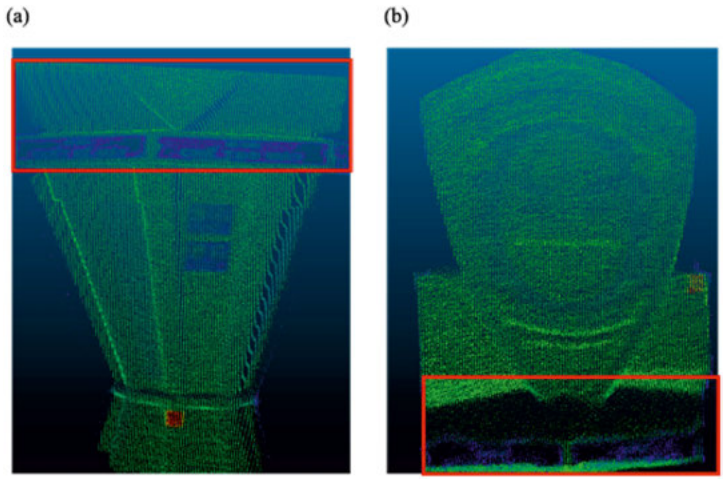

Fig. 6. The point clouds generated from one viewpoint in the case of (a) nadir and oblique scanning. The poor quality in oblique scanning is shown clearly in the overlap area displayed inside the rectangle. A part of the object cannot be visualized correctly

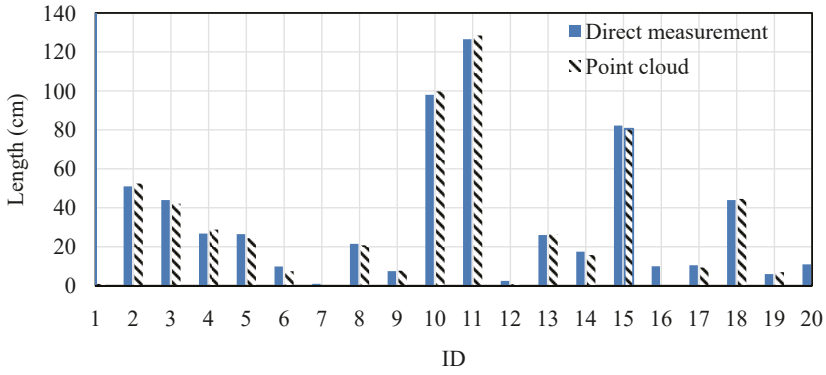

Fig. 7. The comparison of length measured on the point cloud and the object

number 6 (ID = 6) (Fig. 8). This detail locates in the head part of the object is partially hidden from oblique viewing. In particular, the achieved RMSE is approximate ±1.5 cm.

As mentioned above, outliers of each point cloud are manually removed. Thanks to this process, the size of generated point clouds is reduced. It allows the data processing process to be performed faster. Then, the point clouds are aligned for the affine transformation process. Four tie points are selected for each group of two continuous point clouds, and their coordinates are used to compute seven transformed parameters by applying the least square method. The scaling factor in all cases is near 1.0. As a result, the coordinates of all points in the reference point cloud is recomputed into the primary point cloud's coordinate system. The combination of two point clouds leads to the increasing of points at overlap parts. Therefore, duplicated points will be removed for the best quality of the point cloud. Some object features have no

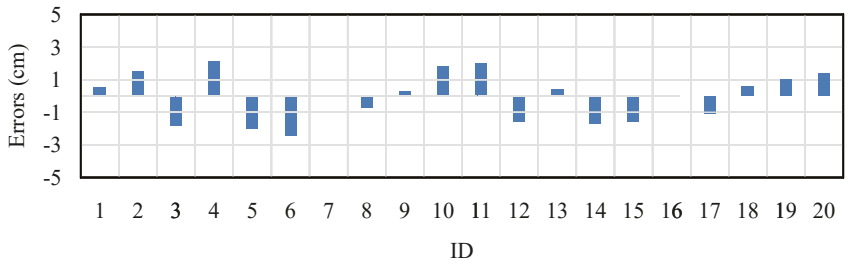

Fig. 8. The error of each measured side

data because the top head portion cannot be captured in nadir and oblique scanning planes. However, the detail in the rest of the model is obvious. In general, the generated 3D point cloud is suitable for a good overview of the object. The generated 3D point cloud combined 16 separated point clouds at eight viewpoints (Fig. 9). It is displayed in a united coordinate system with the false origin located at the device's start point at one of eight viewpoints. As a result, the point cloud contained approximately 1.4 billion points. It is very dense. The corners or small details on the object's surface can be visualized clearly. The corrected point cloud still contains noisy points, especially edge parts and corners. A filter is applied to remove them by using the k-nearest neighbor algorithm to remove the noisy component. However, the noisy points cannot be removed completely.

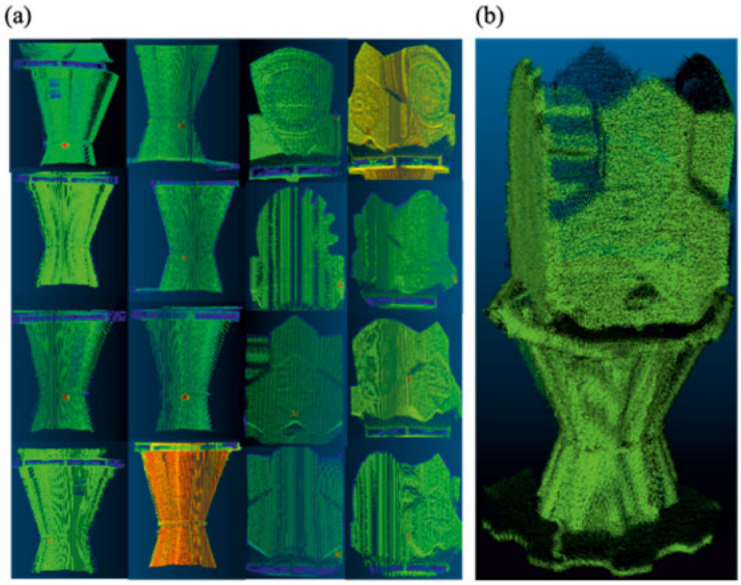

Fig. 9. The generated point cloud of the object. (a) the results from single scans at eight viewpoints; two first columns show the result of nadir scanning, and the rest point clouds are the results of oblique scanning. (b) The combined point cloud is visualizing the object in 3D. The generated point cloud still contains noisy points especially, edge parts and corners

5. Discussion

This study displays the processing of collecting and generating precise 3D point clouds from a non-survey grade laser scanner Hokuyo UTM 30 LX. According to the proposed data processing, a self-developed script in R language generates the point cloud for single scans. As a result, 16 single point clouds were generated from 8 nadir and eight oblique scanning times. Because of the limited length of the rubber rail, at one viewpoint, the device cannot capture the whole face of the object in nadir scanning. Therefore, the oblique scanning was set up to capture the head portion of the object. By applying oblique scanning, the object's parts which higher than the device's installation height could be obtained. Depending on the stability of speed movement and boresight angles, the point-clouds quality is directly influenced.

In comparison, the nadir scanning plane's point cloud has better quality than the one collected in the case of the oblique scanning plane. For instance, in the overlay part of two scans from one viewpoint, the nadir scan displays a clear image. In contrast, many ghost points in oblique scanning make a different visualization of the object (Fig. 6). It affects the quality of the final point cloud. Moreover, some parts cannot be captured because of the oblique direction. This object has many edges and corners, so the ghost points caused by diagonal scanning may affect the generated point cloud's quality. In general, the quality of the point cloud is good, with a dense density of points. Therefore, small details of the object's surface can be visualized clearly. However, in the oblique point cloud, the 3D shape visualized from the point cloud has a slight skew. This is caused by the un-straight of the rail because of the abundance of the ground surface. The mark points on the frame mark the oblique angle. It may lead to incorrect results in measuring the tilted angle. As a result, the effect of oblique scanning cannot be entirely removed by applying the proposed process. The generated point cloud might display a slight skew in the shape of the target object. Moreover, some parts of the object have no data in case of oblique scanning. It clear that the hidden part from the viewpoint cannot be captured. That explains why the quality of oblique point clouds is not so good as nadir point clouds.

The outlier points are then removed manually. As a result, the rest of the points contain the information of the object. However, ghost points appear at the edge parts and corners. It is complicated to remove those noises. Ghost points imply the incorrect position of the scanning point. They lead to distortion in the shape of 3D visualizing from the point cloud. They may affect the point-cloud quality, especially for the subsequent analysis of generating a 3D model automatically from the point cloud. Therefore, to enhance point clouds' quality, it is better to apply methods for removing ghost points. Therefore, a filter is used to empty these ghost points based on the k-nearest neighbor algorithm. Finally, many ghost points are removed.

The combination of 16 single point clouds is a challenge in this study. First, according to the data processing order, two point clouds at the same viewpoint are combined. Then, point clouds at eight viewpoints are combined to get the object's full 3D point cloud in a united coordinate system. For each transformation process, four tie points are chosen for the affine transformation. The least-square method is applied to identify the translation, scale, and rotation parameters. The chosen tie point's position affects the accuracy of the transformation process; therefore, this step has to be performed many times. Cross-sections at the overlapping portion are checked to make sure that two-point clouds were matched entirely. All computed scaling factors are approximate 1.0. This result confirms that all point clouds were generated at the

same scale despite different viewpoints. Each point cloud consists of approximately 280.000 points. After removing the outliers and doing combinations, the resulting point cloud consists of 1.4 billion points (object only) and represents the object in 3D with great detail. The scan point reflectance intensity depends on the position, angle of incidence, and material surface. Therefore, the difference in reflection intensity makes the details on the point cloud more clearly visible. In detail, the small part of the object can be shown clearly, such as bumps on the surface of the body or head part. Their size can be measured directly on the point cloud. For instance, ridges of 1 cm high on object's surface can be visually identified on the point cloud. Moreover, the small character can be read (Fig. 6). The geometric shape of the object in the cloud is similar to its actual form. Only minor distortions are detected in the clouds obtained from the oblique scan. However, this has a negligible effect on the quality of the resulted point cloud. This technique mentioned in this study is good for getting more detailed information on the object's surface. For direct measurement, it very difficult to collect such detailed information. A comparison with the measured data is performed to analyze its geometrical accuracy. The most considerable variations of 2.4 cm can be found at the head of the object. Based on the analysis results, most of the significant geometrical errors are in the head of the object, where it is recorded by oblique observations (Fig. 8). There are two measurement positions (ID = 7 and ID = 16) that cannot be determined on the model due to being obscured by the oblique scan. Most of the samples measured in other parts have minor geometric errors with approximately 1 cm of magnitude. This confirms that the quality of the oblique point clouds is not so good as that of the nadir point clouds. In general, the resulted point cloud is achieved with the deviations RMSE of ± 1.5 cm. The generated result is valuable input data for further data processing to develop a 3D model. The quality of the point cloud is also sufficient for measurements in the object and for building reconstruction. In detail, we can measure the size of any part of the object and compare the directly-measured data for checking. Beyond measuring the point cloud, it is possible to use the point cloud for visual inspection, such as detecting an object or visualizing the old construction's newly designed parts.

Besides the above-mentioned achievements, this study's main problem is missing data and ghost points in oblique scanning. For this, it better to develop a system for capturing data in nadir scanning only. The limited length of the rail reduces the flexibility of data collection. It is better to attach the device on a more flexible platform than a frame. A UAV-based laser scanner is an expected system. The laser scanner used in this system is a low-weight device. It is possible to attach this device to a low-cost UAV for collecting data. The data processing for this process is complicated; However, the device can capture complete information of the object. In general, the resulting point cloud in this study is sufficient to give an overview of the measured object, and the measurement can be made directly on the point cloud. Moreover, it can automatically generate the 3D model of an object by applying many structure analyses.

On the other hand, it takes time for data processing. There is no business software for processing the raw data collected by a 2D laser scanner. Therefore, it needs to develop the script for generating the point cloud from the raw file before using open-source software for the point cloud analysis. The low-cost device and open-source software can be considered as a solution for using laser scanners for small projects with the narrow economic resources in developing countries.

6. Conclusion

This study has confirmed the ability to generate a 3D point cloud from this non-grade surface laser scanner. In detail, this paper presents the generation of 3D point clouds based on data from a 2D laser scanner, the Hokuyo UTM 30LX. Processing data processing from raw data (*.uhb file) to the 3D object points is done by a self-developed R script based on the proposed data processing process. The resulting 3D point cloud combined from 16 single point clouds consists of 1.4 million points (object only) and represents the object in great detail. This result shows the ability to combine nadir and oblique scanning to capture and visualize 3D objects using a 2D scanner. The resulting point cloud is dense in clarity and detail. Its geometrical accuracy is analyzed by comparing it with the measured data. As a result, the maximum absolute deviation is 2.4 cm. The RMSE is approximate ± 1.5 cm. From this result, we can also reconstruct the object's 3D model for other purposes, such as making a copy. Moreover, the expert can check the object's current quality directly on the 3D point cloud or with a visual inspection, such as damage detection. The quality of the point cloud is also sufficient for measuring purposes; however, the 3D point cloud's quality depends directly on the device's stability when it is moving. The limitation of the rail length is an opposing point of this system in this study. Oblique scanning is not as good as nadir scanning because of lacking information. It is soon better to develop a mobile laser scanning system for flexible collect data in nadir scanning. Moreover, UAV – based laser scanning system is a good idea for collecting information from above. From this, the experts can be indirectly testing the quality of construction. Although data processing takes time, the low-cost 2D laser scanner is suitable for a small project in developing countries. By combining with photogrammetry, this system can support the data have good quality enough for checking purposes the quality of in-built or built construction.

Acknowledgements

The research work presented in this paper has been funded by Ho Chi Minh City University of Technology-VNU-HCM under grant number To-KTXD-2019-04.

References

[1] A. Berenyi, T. Lovasand, and A. Barsi, "Terrestrial laser scanning – civil engineering applications, International Archives of Photogrammetry". Remote Sensing and Spatial Information Sciences, vol. 38, Part 5, Commission V Symposium, Newcastle upon Tyne, UK. 2010.

[2] M. Dassot, T. Constantand, and M. Fournier, "The use of terrestrial LiDAR technology in forest science: application fields, benefits and challenges". Annals of Forest Science, vol. 68, pp. 959–974, 2010, DOI: 10.1007/s13595-011-0102-2.

[3] R. Thakur, "Scanning LIDAR in advanced driver assistance systems and beyond: Building a road map for next-generation LIDAR technology". in IEEE Consumer Electronics Magazine, vol. 5, no. 3, pp. 48–54, July 2016.

[4] Y. Yin and Y. Antonio, "Application of 3D laser scanning technology for image data processing in the protection of ancient building sites through deep learning". Image and Vision Computing, vol. 102, 2020, DOI: 10.1016/j.imavis.2020.103969.

[5] J. Balsa-Barreiro and D. Fritsch, "Generation of visually aesthetic and detailed 3D models of historical cities by using laser scanning and digital photogrammetry". Digital Applications in Archaeology and Cultural Heritage, vol. 8, pp. 57–64, 2018, DOI: 10.1016/j.daach.2017.12.001.

[6] R. Napolitano, M. Hessand, and B. Glisic, "Integrating non-destructive testing, laser scanning, and numerical modeling for damage assessment: the room of the elements". Heritage, vol. 2, pp. 151–168, 2019, DOI: 10.3390/heritage2010012.

[7] Y.Y. Su, Y.M.A. Hashashand, and L. Y. Liu, "Integration of construction as-built data via laser scanning with geotechnical monitoring of urban excavation". Journal of Construction Engineering and Management, vol. 132, no. 12, 2006.

[8] E.S. Park and H.C. Seo, "Risk analysis for earthquake-damaged buildings using point cloud and BIM data: a case study of the Daeseong apartment complex in Pohang, South Korea". Sustainability, vol. 13, no.2, p. 456, 2021, DOI: 10.3390/su13020456.

[9] F. Bosché, et al., "The value of integrating Scan-to-BIM and Scan-vs-BIM techniques for construction monitoring using laser scanning and BIM: The case of cylindrical MEP components". Automation in Construction, vol. 49, part B, pp. 201–213, 2015, DOI: 10.1016/j.autcon.2014.05.014.

[10] D. Rebolj, et al., "Point cloud quality requirements for Scan-vs-BIM based automated construction progress monitoring". Automation in Construction, vol. 84, pp. 323–334, 2017, DOI: 10.1016/j.autcon.2017.09.021.

[11] G. Rocha, et al., "A Scan-to-BIM methodology applied to heritage buildings". Heritage, vol. 3, no. 1, pp. 47-67, 2020, DOI: 10.3390/heritage3010004.

[12] M.E. Esfahani, et al., "Quantitative investigation on the accuracy and precision of Scan-to-BIM under different modelling scenarios". Automation in Construction, vol. 126, 2021.

[13] Q. Wangand and M.K. Kim, "Applications of 3D point cloud data in the construction industry: A fifteen-year review from 2004 to 2018". Advanced Engineering Informatics, vol. 39, pp. 306–319, 2019.

[14] T. Wang and Z. Xiong, "Methods of As-is BIM reconstruction using point cloud data for existing buildings". IOP Conference Series: Earth and Environmental Science, Bristol, vol. 676, no. 1, 2021.

[15] Y. He, et al., "Real-time 3D reconstruction of thin surface based on laser line scanner". Sensors, vol. 20, no. 2, p. 534, 2020, DOI: 10.3390/s20020534.

[16] A.A. Al-Temeemyand S.A. Al-Saqal, "Laser-based structured light technique for 3D reconstruction using extreme laser stripes extraction method with global information extraction". Optics and Laser Technology, vol. 138, 2021, DOI: 10.1016/j.optlastec.2020.106897.

[17] F. Javadnejad, et al., "Dense point cloud quality factor as proxy for accuracy assessment of image-based 3D reconstruction". Journal of Surveying Engineering, vol. 147, no. 1, February 2021.

[18] J.C. White, et al., "Comparing ALS and image-based point cloud metrics and modelled forest inventory attributes in a complex coastal forest environment". Forests, vol. 6, no. 10, 2015, DOI: 10.3390/f6103704.

[19] J.L.R. Jensen and A.J. Mathews, "Assessment of image-based point cloud products to generate a bare earth surface and estimate canopy heights in a woodland ecosystem". Remote Sens, vol. 8, no. 1, p. 50, 2016, DOI: 10.3390/rs8010050.

[20] F. Javadnejad, et al., "A photogrammetric approach to fusing natural colour and thermal infrared UAS imagery in 3D point cloud generation". International Journal of Remote Sensing, vol. 41, no. 1, pp. 211–237, 2020.

[21] G. Karakas, et al., "Derivation of earthquake-induced landslide distribution using aerial photogrammetry: the January 24, 2020, Elazig (Turkey) earthquake". Landslides, vol. 18, pp. 2193–2209, 2021, DOI: 10.1007/s10346-021-01660-2.

[22] N. Cenni, S. Fiaschi, and M. Fabris, "Integrated use of archival aerial photogrammetry, GNSS, and InSAR data for the monitoring of the Patigno landslide (Northern Apennines, Italy)", Landslides, vol. 18, 2021, DOI: 10.1007/s10346-021-01635-3.

[23] A. Guarnieri, N. Milanand , and A. Vettore, "Monitoring of complex structure for structural control using Terrestrial Laser Scanning (TLS) and photogrammetry". International Journal of Architectural Heritage, vol. 7, no. 1, pp. 54–67, 2013.

[24] I. Aicardi, et al., "Integration between TLS and UAV photogrammetry techniques for forestry applications". iForest vol. 10, no. 1, pp. 41–47, 2016.

[25] F. Alidoost and H. Arefi, "Comparison of UAS-based photogrammetry software for 3D point cloud generation: a survey over a historical site". ISPRS Annals of the Photogrammetry, Remote Sensing and Spatial Information Sciences, vol. IV-4/W4, the 4th International GeoAdvances Workshop, Safranbolu, Karabuk, Turkey, 14–15 October 2017.

[26] D. Moon, et al., "Comparison and utilization of point cloud generated from photogrammetry and laser scanning: 3D world model for smart heavy equipment planning". Automation in Construction, vol. 98, pp. 322–331, 2019.

[27] G. Kermarrec, B. Kargolland, and H. Alkhatib, "Deformation analysis using B-spline surface with correlated terrestrial laser scanner observations – a bridge under load". Remote Sens, vol. 12, no. 5, p. 829, 2020, DOI: 10.3390/rs12050829.

[28] K. Tan, et al., "Estimation of soil surface water contents for intertidal mudflats using a near-infrared long-range terrestrial laser scanner". ISPRS Journal of Photogrammetry and Remote Sensing, vol. 159, pp. 129–139, 2020, DOI: 10.1016/j.isprsjprs.2019.11.003.

Received: 2021-04-26, Revised: 2021-07-07